AMERICAN SOCIETY FOR MICROBIOLOGY | Antimicrobial Agents and Chemotherapy

8-Hydroxyquinolines Are Boosting Agents of Copper-Related Toxicity in *Mycobacterium tuberculosis*

Santosh Shah,[a] Alex G. Dalecki,[a] Aruni P. Malalasekera,[c] Cameron L. Crawford,[a] Suzanne M. Michalek,[b] Olaf Kutsch,[a] Jim Sun,[a] Stefan H. Bossmann,[c] Frank Wolschendorf[a]

Department of Medicine, Division of Infectious Diseases,[a] and Department of Microbiology,[b] University of Alabama at Birmingham, Birmingham, Alabama, USA; Department of Chemistry, Kansas State University, Manhattan, Kansas, USA[c]

Copper (Cu) ions are likely the most important immunological metal-related toxin utilized in controlling bacterial infections. Impairment of bacterial Cu resistance reduces viability within the host. Thus, pharmacological enhancement of Cu-mediated antibacterial toxicity may lead to novel strategies in drug discovery and development. Screening for Cu toxicity-enhancing antibacterial molecules identified 8-hydroxyquinoline (8HQ) to be a potent Cu-dependent bactericidal inhibitor of *Mycobacterium tuberculosis*. The MIC of 8HQ in the presence of Cu was 0.16 μM for replicating and nonreplicating *M. tuberculosis* cells. We found 8HQ's activity to be dependent on the presence of extracellular Cu and to be related to an increase in cell-associated labile Cu ions. Both findings are consistent with 8HQ acting as a Cu ionophore. Accordingly, we identified the 1:1 complex of 8HQ and Cu to be its active form, with Zn, Fe, or Mn neither enhancing nor reducing its Cu-specific action. This is remarkable, considering that the respective metal complexes have nearly identical structures and geometries. Finally, we found 8HQ to kill *M. tuberculosis* selectively within infected primary macrophages. Given the stark Cu-dependent nature of 8HQ activity, this is the first piece of evidence that Cu ions within macrophages may bestow antibacterial properties to a Cu-dependent inhibitor of *M. tuberculosis*. In conclusion, our findings highlight the metal-binding ability of the 8-hydroxyquinoline scaffold to be a potential focus for future medicinal chemistry and highlight the potential of innate immunity-inspired screening platforms to reveal molecules with novel modes of action against *M. tuberculosis*.

The ability to provide and administer effective treatment to patients with tuberculosis (TB) disease is an essential component of global control efforts and, in retrospect, has had a tremendous impact on controlling TB prevalence and reducing the incidence of TB and the rates of mortality from TB (1). However, these major accomplishments are threatened by drug-resistant *Mycobacterium tuberculosis* strains, estimated to be responsible for up to 5% (480,000) of the 9.6 million annual TB cases worldwide (1). Of particular worry is the fact that in some countries, up to 34% of new cases and up to 69% of recurring infections are already classifiable as multidrug-resistant (MDR) TB (1). Unfortunately, the efficacy and therapeutic qualities of current MDR TB treatments do not match those of the standard first-line regimen of isoniazid, ethambutol, rifampin, and pyrazinamide, reflected in part by an only ~50% treatment success rate within the global cohort with MDR TB (1). Therefore, new drugs are urgently needed to ensure the future success of TB treatment and control programs.

Repurposing of existing drugs with known pharmacological properties is one of the most economical and fastest strategies for drug discovery and development. One such promising molecule with a broad spectrum of activity and a high repurposing potential is 8-hydroxyquinoline (8HQ) (2). The activity of 8HQ and several of its derivatives against *M. tuberculosis* has already been investigated *in vitro* (3, 4) and was successfully tested in both animal models (5) and humans (6). More recently, high-throughput screening against *M. tuberculosis* in culture identified 8HQ derivatives to be a major hit cluster, with more than 200 analogues being active within a concentration range of from 0.1 to 50 μg/ml. Remarkably, some of the compounds produced *in vitro* therapeutic indices of up to 100 when tested against eukaryotic Vero cells (7). Other desirable properties of halogenated or nonhalogenated 8HQ derivatives include a bactericidal mode of action, activity against nonreplicating *M. tuberculosis* cells, and potency against monoresistant and multidrug-resistant clinical *M. tuberculosis* isolates (8). In addition, 8-hydroxyquinoline-2-carboxylic acid (HCA) has been identified to be a potent noncompetitive inhibitor of the *M. tuberculosis* class IIa fructose 1,6-bisphosphate aldolase, which is a well-characterized pathogen-specific drug target (9).

A common trait of 8HQs is their affinity for metal ions, which is critical for their *in vitro* antibacterial properties toward most Gram-positive and Gram-negative organisms (10–13). The power of 8HQ chelation with physiologically relevant bivalent metal ions essentially follows the Irving-Williams series of metal complex stabilities (14) (Zn < Cu > Co > Fe > Mn), according to which Cu ions form the most stable complexes. However, the type of the 8HQ-metal complex that forms in a given system depends heavily on the metal ion (M)-to-ligand (L) ratio (12). In the presence of excess ligand, a 1:2 complex (ML_2) forms, while in the presence of excess metal ion, a complex with a 1:1 (ML) stoichiometry prevails (12). In addition, pH, temperature, ring adornments, and the

Received 9 February 2016 **Returned for modification** 6 March 2016
Accepted 6 July 2016

Accepted manuscript posted online 18 July 2016

Citation Shah S, Dalecki AG, Malalasekera AP, Crawford CL, Michalek SM, Kutsch O, Sun J, Bossmann SH, Wolschendorf F. 2016. 8-Hydroxyquinolines are boosting agents of copper-related toxicity in *Mycobacterium tuberculosis*. Antimicrob Agents Chemother 60:5765–5776. doi:10.1128/AAC.00325-16.

Address correspondence to Frank Wolschendorf, fwolsche@uab.edu.

Supplemental material for this article may be found at http://dx.doi.org/10.1128/AAC.00325-16.

basicities of the oxygen and nitrogen donor atoms are known to influence the solubility, hydrophobicity, and/or stability of 8HQ-metal complexes (15).

Although the impact of metal ion chelation on the *in vivo* performance of 8HQ and its derivatives remains to be established, recent research has revealed an intriguing novel opportunity to potentially utilize metal-chelating agents for anti-infective therapy. Multiple studies suggest that the innate immune system facilitates the accumulation of Cu ions at the site of infection, thereby exploiting Cu ions as a natural antimicrobial agent (16–18). Our laboratories previously reported elevated Cu levels in *M. tuberculosis*-infected lung tissue of guinea pigs (18). Such infected tissue is often hypoxic (19) and usually infiltrated by macrophages (20). Interestingly, hypoxia stimulates expression of ATP7A (21–23), a Cu-transporting P-type ATPase present in most eukaryotes (including humans). In activated macrophages, ATP7A translocates to the phagosome (16, 23), in which trapped mycobacteria can experience Cu concentrations of up to 400 μM (17). Consistent with this model, *M. tuberculosis*-Cu homeostasis and resistance genes are induced in macrophages (24) and animal infection models (25), while impairment of these pathways reduces *M. tuberculosis* virulence (18, 26, 27).

As Cu ions accumulate at the site of infection, compounds that gain significant antibacterial properties in such Cu-rich environments may enable pharmacological control of Cu's antibacterial potency right at the site of infection. As the ability of 8HQ and many of its derivatives to bind Cu ions can enhance its antimicrobial properties (10–13, 28), derivatives may be ideally suited to probe the related chemical space for potential metal-dependent activities. However, a potential synergy between Cu or other physiologically relevant transition metal ions and the activity of 8HQs on *M. tuberculosis* is unknown and, to our surprise, was not elucidated in previous studies (3, 8). Given the consideration of 8HQ as an established scaffold for the development of novel antimycobacterial agents (2, 8) and the omnipresence of Cu ions *in vivo* (29, 30), it is imperative to detail and understand the impact of transition metal ions on the activity of 8HQs against *M. tuberculosis*.

In this study, we deconstruct the activity profile of 8HQ against *M. tuberculosis* and demonstrate that Cu ions are indispensable for *in vitro* inhibition. We characterize the active component to be a 1:1 ligand-ion complex that is able to form under likely therapeutic conditions and that is efficacious even in the presence of other transition metals. Finally, we employed 8HQ in a macrophage infection model and for the first time provide evidence that a Cu-dependent inhibitor is able to synergize with the Cu-burst action of the innate immune system.

MATERIALS AND METHODS

Chemicals and reagents used in biological assays. Metal salts for biological assays ($ZnCl_2$, $MnCl_2$, $CuCl_2$, $CuSO_4$) were all purchased from Sigma and solubilized in double-distilled H_2O. Aliquots of 100 mM stock solutions were stored at 4°C. $FeCl_2$ (Fisher) solution was always prepared fresh. 8HQ (Sigma), clioquinol (CQ; Sigma), nitroxoline (NQ; Sigma), and HCA (Fisher) were solubilized in sterile dimethyl sulfoxide (Sigma) and stored in small 10 mM aliquots at −80°C. The purity of the organic compounds was ascertained by using ^1H and ^{13}C nuclear magnetic resonance spectroscopy. They were found to be more than 95% pure. For determination of metal complex formation constants, American Chemical Society (ACS)-grade $CuBr_2$ and $ZnSO_4$ were purchased from Aldrich. Fluorescein diacetate (FDA) was purchased from Sigma.

Mycobacterial strains and standard growth conditions. *Mycobacterium smegmatis* strains SMR5 (wild type) (31), ML16 (an SMR5 derivative from which porins were deleted, SMR5 Δ*mspA* Δ*mspC* Δ*mspD*) (32), and ML16/pMN016 (an *mspA*-expressing ML16 derivative) (32) and *Mycobacterium tuberculosis* strains H37Rv (wild type) and mc^26230 (an H37Rv Δ*panCD* Δ*RD1* derivative) (33) were grown in Middlebrook 7H9 medium ($7H9_{MB}$; BD, Difco) or copper sulfate-free Hartmans-de Bont (HdB) minimal medium (HdB_{SM}) (34) or plated on Middlebrook 7H10 agar (BD, Difco). The base composition of HdB_{SM} is as follows: 15 mM $(NH_4)_2SO_4$, 6 mM K_2HPO_4, 6 mM NaH_2PO_4, 1% glycerol, 0.5% glucose, 30 μM EDTA, 500 μM $MgCl_2$, 7 μM $CaCl_2$, 0.8 μM Na_2MoO_4, 1.68 μM $CoCl_2$, 5.49 μM $MnCl_2$, 6.95 μM $ZnSO_4$, and 20 μM $FeSO_4$. Copper sulfate-free 7H9 medium ($7H9_{SM}$) was prepared from scratch by excluding copper salt from the Middlebrook medium recipe. All growth media were supplemented with hygromycin (50 μg/ml; BD), 10% oleic acid-albumin-dextrose-catalase (OADC) supplement (BD Middlebrook), pantothenate (pan; 24 μg/ml), 0.02% tyloxapol, or combinations thereof as required.

Dose-response curves for MIC determination. Multidose-response curves were generated as described previously (35). Briefly, bacteria were grown in HdB_{SM}. *M. smegmatis* strains were grown overnight, and *M. tuberculosis* strains were grown for up to 14 days to an optical density at 600 nm (OD_{600}) that did not exceed 2.0. Cells were diluted to an OD_{600} of 0.04 in 2-fold-concentrated medium right before the assay was performed. Compounds were diluted 2-fold down from 10 μM in 96-well plates in either water or metal salt solutions to reach the concentrations indicated below. An equal volume of 2-fold-concentrated HdB medium with cells was then added to each well. Unless stated otherwise, the final copper sulfate content per well was 10 μM for *M. smegmatis* or 7.5 μM for *M. tuberculosis* in HdB medium. For the medium discrepancy assay, either a homemade copper sulfate-free 7H9 medium ($7H9_{SM}$) or commercial 7H9 Middlebrook medium (which already contains ~6 μM copper sulfate) was used, with Cu-positive wells having additional 6 μM copper sulfate present. For metal specificity assays, 7.5 μM metal chlorides were added to the base HdB_{SM}. No differences between the use of $CuCl_2$ and $CuSO_4$ in biological assays were noted (compare the MIC of Cu combined with 8HQ from Fig. 1D and 2A). In the case of metal competition assays, Cu was provided at 7.5 μM and the competing metals were provided at an additional 20 μM each, unless stated otherwise. To determine the metal sensitivity of *M. tuberculosis* mc^26230, only the indicated metal salts were 2-fold serially diluted in HdB_{SM}, with the highest concentration being 1 mM. Assay mixtures with *M. smegmatis* were incubated for 16 to 24 h at 37°C. The incubation period for all *M. tuberculosis* strains was 7 days. Thereafter, resazurin dye was added to a final concentration of ~90 μM resazurin. Resazurin (blue) is converted to resorufin (pink) by viable bacteria over the course of several hours. The fluorescence intensity of resorufin (excitation wavelength, 560 nm; emission wavelength, 590 nm) was determined on a Cytation3 imaging reader (BioTek) and analyzed using Gen5 software (BioTek), Microsoft Excel 2010 software, and GraphPad Prism (v7) software. All conditions were analyzed in triplicate, and all experiments were repeated at least once. Plates also contained a medium-only control to determine background dye conversion in the absence of cells and a no-treatment condition to determine dye conversion rates under optimal growth (100% growth). The results for all data points were normalized to those for plate-specific controls. The MIC was defined as the lowest concentration effecting a reduction in fluorescence of ≥85% relative to the mean for non-drug-treated bacterium-only controls.

Time-to-kill studies. Cells from a growing culture were harvested and treated in the presence or absence of 7.5 μM $CuSO_4$ with 0.6 μM 8HQ or NQ in HdB_{SM} at 37°C. The OD_{600} of the samples was 0.04. Aliquots were removed at the indicated treatment times. The samples were then diluted 10-fold in $7H9_{SM}$. Aliquots (5 μl) of each dilution were spotted on 7H10 agar plates and incubated at 37°C for 11 days before pictures were taken.

Dose matrix experiments. Serial dilutions (2-fold) of $CuCl_2$ or $ZnCl_2$ were carried out at 4-fold concentrations in 96-well plate rows, and one-

fourth of the total volume of each well was filled with these dilutions. Test compound was diluted separately in a 12-well reservoir at 4-fold concentrations, and then one-fourth volume of each well was added into the wells of the respective columns containing the metal solutions or water, giving rise to a dose matrix. Finally, one-half volume of 2-fold-concentrated HdB_{SM} with cells (OD_{600} = 0.04) was added to each well. The final concentrations of Cu and compounds are given in the appropriate figures. Plates were incubated at 37°C for 7 days, after which the resazurin assay was used to determine the growth of the cells by measuring the fluorescence intensity using a Cytation3 imaging reader (BioTek). Data were analyzed using Gen5 software (v2.07; BioTek), Microsoft Excel 2010 software, and GraphPad Prism (v7) software.

Generation of nonreplicating *M. tuberculosis* mc^{2}6230 cells. Nonreplicating cells were prepared as described elsewhere with some modifications (36). Briefly, the strain was grown in Middlebrook 7H9 medium with 10% OADC (BD Middlebrook), pan (24 μg/ml), and 0.02% tyloxapol for 7 days to an OD_{600} of >2. The cells were harvested by centrifugation (30 min at 3,500 × *g*), washed three times with phosphate-buffered saline (PBS) buffer (pH 7.4) containing pan (24 μg/ml) and 0.02% tyloxapol, and then resuspended in 50 ml of the same buffer. Incubation at 37°C continued for at least 6 weeks. Then, the cells were harvested by centrifugation (30 min at 3,500 × *g*) and resuspended in fresh $7H9_{SM}$ for treatment with various concentrations of 8HQ in the presence or absence of 7.5 μM copper sulfate. The inoculum for nonreplicating cells gave an OD_{600} of 0.04 when all components were added to the wells. Other than that, the assay was performed like a standard dose-response assay, as described above. In addition, before addition of resazurin to the wells, the samples were mixed, and 5 μl was removed and immediately spotted on Middlebrook 7H10 agar plates. The agar plates were incubated at 37°C for an extra 11 days before pictures were taken.

PGFL assay. The previously developed PhenGreen FL (PGFL) assay (37) was used to determine the treatment-dependent alterations of the labile cellular metal content. Mycobacteria were grown in Cu-free HdB_{SM}, washed once in the same medium, adjusted to an OD_{600} of 1.0, and then treated with the concentrations of compound and/or copper sulfate indicated below for 2 h at 37°C. Thereafter, cells were washed once in PBS (pH 6.8) containing 500 μM EDTA and 0.02% tyloxapol and then twice in PBS with tyloxapol and were then resuspended in the same buffer to give an OD_{600} of 1. A 100-μl aliquot of each sample was transferred into 96-well plates in triplicate, and PGFL solution was added to give a final concentration of 2.5 μM. After 30 min of incubation, fluorescence (excitation wavelength, 490 nm; emission wavelength, 520 nm) was measured on a Cytation3 imaging reader (BioTek), controlled by Gen5 software, and analyzed using Microsoft Excel 2010 software and GraphPad Prism (v7) software.

Fluorescein diacetate viability staining of *M. tuberculosis* and flow cytometry. Fluorescein diacetate requires metabolic conversion to fluorescein in order to become fluorescent. Only metabolically active *M. tuberculosis* cells are able to perform this conversion. Therefore, the accumulation of fluorescence is a measure of the vital state of individual cells without the need to rely on cellular multiplication (38). We essentially followed the staining procedure described previously (38, 39). Briefly, *M. tuberculosis* mc^{2}6230 cells were harvested from cultures by centrifugation, resuspended in HdB_{SM} or RPMI 1640 medium supplemented with 10% heat-inactivated fetal bovine serum (FBS) and *M. tuberculosis* mc^{2}6230-specific supplements (tyloxapol, pan) to an OD_{600} of 0.04, and treated with 1 or 10 μM 8HQ for 48 h at 37°C. Where indicated, $CuSO_4$ was added to a final concentration of 7.5 μM. Then, 25 μl was removed, transferred into a fresh 96-well plate, and mixed with 2.5 μl FDA solution to give a final FDA concentration of 500 ng/ml. After 1 h of incubation at 37°C, staining was stopped by adding 200 μl PBS with 0.02% tyloxapol to each well. Samples were analyzed on a Guava EasyCyte flow cytometer (Guava Technologies, Inc.) using the green fluorescent channel. The flow cytometer was controlled by CytoSoft (v5.3) software (Guava Technologies, Inc.). Data were analyzed and graphed using Microsoft Excel software.

Determination of metal complex formation constants. For determination of metal complex formation constants, ACS-grade $CuBr_2$ and $ZnSO_4$, purchased from Aldrich, were used. Stock solutions of 8HQ, CQ, NQ, HCA, and the metal salts were prepared in HEPES buffer, pH 7.4 (100 μM for the organic compounds, 10 μM for the metal cations), and kept under argon. All UV-visible titration experiments were performed at 25°C using a Varian Cary 500 UV–visible–near-infrared spectrophotometer in 4.0-ml quartz cuvettes. The ratios of metal cations and organic ligands were preoptimized using the BINDSIM tool on www.supramolecular.org, which is an online tool for supramolecular research and analysis provided by the ARC Centre of Excellence in Convergent Bio-Nano Science & Technology, University of New South Wales, Australia (www.supramolecular.org) (40, 41). The fitting of the data was performed by utilizing the L-BFGS-B algorithm, which is available on the website (42). The calculations assume that complexation between the metal (M) and the ligand (L) proceeds in two consecutive steps (see reactions I and II), with the partial formation constants (k_1 and k_2) and the overall formation constant (K_f) being defined as shown in equations 1 to 3, respectively. The maximal errors of all measurements/calculations were <5% for k_1, <3% for k_2, and <15% for K_f. The BINDSIM tool was also used to calculate the mole fractions of L, ML, and ML_2, shown in Fig. S6A to C in the supplemental material, from determined values (see Table S2 in the supplemental material) or previously published values for k_1 (12).

$$M + L \xrightarrow{k_1} ML \qquad \text{(reaction I)}$$

$$ML + L \xrightarrow{k_2} ML_2 \qquad \text{(reaction II)}$$

$$k_1 = \frac{[ML]}{[M][L]} \qquad (1)$$

$$k_2 = \frac{[ML_2]}{[ML][L]} \qquad (2)$$

$$K_f = k_1 k_2 \qquad (3)$$

Cytotoxicity assay on peritoneal macrophages using resazurin. Peritoneal macrophages were seeded at 60,000 cells per well in 96-well plates and grown in RPMI 1640 medium (Gibco) supplemented with 10% fetal bovine serum and 1% penicillin-streptomycin-glutamine in a 5% CO_2 environment at 37°C. Drugs and metals were added at the concentrations indicated below. To determine the Cu-related toxicity of the drugs on eukaryotic cells, compounds were diluted in RPMI 1640 medium supplemented with 10% fetal bovine serum and 1% penicillin-streptomycin-glutamine and then transferred into the wells containing cells. The plates were incubated at 37°C in a 5% CO_2 incubator for up to 48 h. Resazurin dye was added to each well at a final concentration of ~90 μM. After continued incubation for ~6 h, microscopic pictures were taken (magnification, ×20) and the fluorescence of the metabolically converted resazurin dye was quantified using a Cytation3 imaging reader (BioTek) and its accompanying Gen5 software.

Macrophage infection assay. Mouse peritoneal macrophages were isolated from female C57BL/6 mice as previously described (35, 43). Approval for the use of mice for the generation of peritoneal macrophages was granted by the University of Alabama at Birmingham's Institutional Animal Care and Use Committee (animal project number IACUC-08560) under full compliance with applicable institutional and NIH policies. Macrophages were seeded at a density of 60,000 per well in 96-well plates and allowed to adhere and rest for 3 days. Then, macrophages were infected with *M. tuberculosis* mc^{2}6230 at a multiplicity of infection of 1:1 (using a conversion factor in which an OD_{600} of 1 is equal to 3×10^8 bacteria) in RPMI 1640 medium supplemented with 10% heat-inactivated FBS for 4 h at 37°C. After three washes to remove extracellular *M. tuberculosis*, the wells were replenished with fresh medium in the absence and presence of 1 or 10 μM 8HQ. Thereafter, at 0 and 48 h postinfection, macrophages were lysed using 200 μl 0.025% SDS to release intracellular *M. tuberculosis*. The macrophage lysate was serially diluted in complete 7H9 medium and plated on 7H10 agar plates supplemented with 24

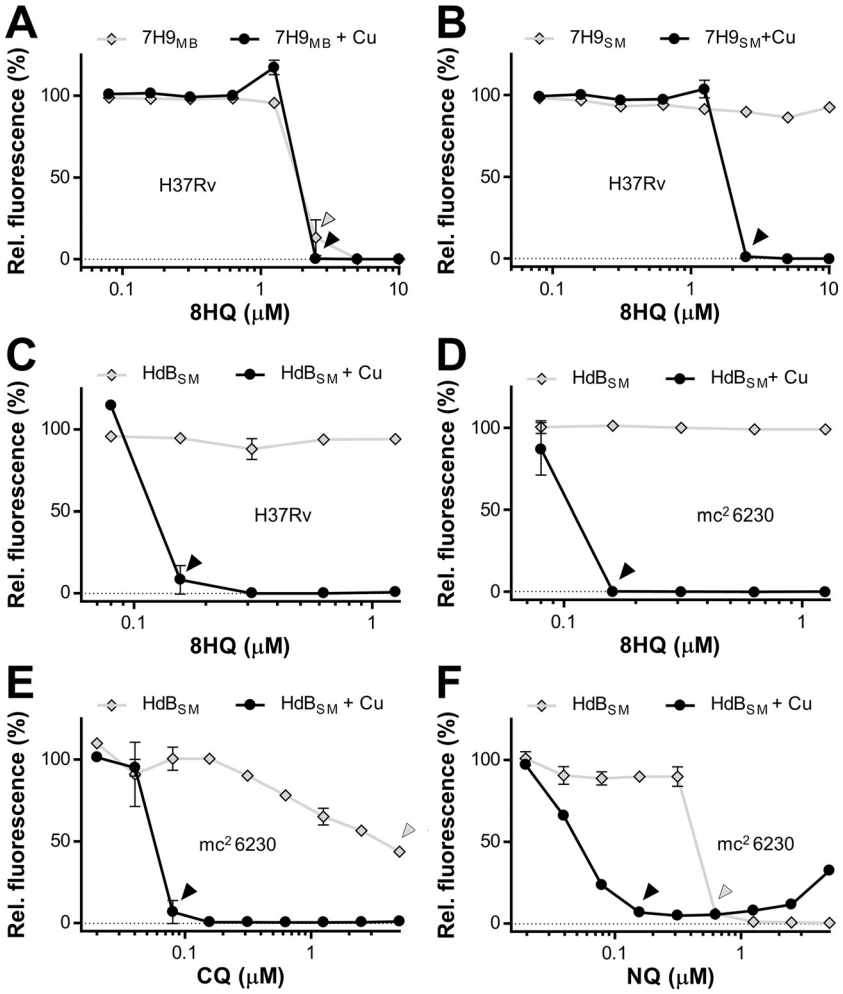

FIG 1 Copper-dependent activity of 8HQ on *Mycobacterium tuberculosis* H37Rv or mc^{2}6230 (Δ*RD1* Δ*panCD*). (A and B) *M. tuberculosis* H37Rv was treated with 8HQ with or without addition of copper sulfate ($CuSO_4$) at 6 μM in either commercial Middlebrook 7H9 medium ($7H9_{MB}$) (A) or homemade $CuSO_4$-free 7H9 medium ($7H9_{SM}$) (B). (C and D) The experiment was then repeated using $CuSO_4$-free HdB_{SM} with or without supplementation with 7.5 μM $CuSO_4$ to compare the activities on *M. tuberculosis* H37Rv (C) and *M. tuberculosis* mc^{2}6230 (D). (E and F) The 8HQ derivatives CQ (E) and NQ (F) were then tested under similar conditions on *M. tuberculosis* mc^{2}6230 in HdB_{SM}. Arrowheads, the MICs of compounds in the presence (black) or absence (gray) of added $CuSO_4$ to highlight Cu-dependent or Cu-independent antibacterial activity. Data sets are representative of those from at least three independent assays conducted under similar conditions. Data points represent the averages from at least three replicates from which the background value was subtracted, with error bars indicating standard deviations. Rel., relative.

μg/ml pantothenic acid. The plates were incubated at 37°C for 14 days, and the number of CFU was counted.

RESULTS

The antimycobacterial activity of 8-hydroxyquinoline is copper dependent. Most reported bioactivities of 8HQ (see Fig. S1A in the supplemental material) are linked to its metal-chelating properties, except for its activity against *M. tuberculosis* H37Rv, where its mode of action was explicitly reported to be metal independent (8). However, a limited copper complexation screen conducted in our laboratories (35, 44) indicated that its activity is strongly enhanced by copper (Cu) ions. Given this discrepancy, we reevaluated the activity of 8HQ toward *M. tuberculosis* H37Rv and its auxotroph surrogate, mc^{2}6230. We first confirmed activity in standard Middlebrook 7H9 medium. In agreement with previous reports (8), the MIC was 2.5 μM (Fig. 1A). However, as Middlebrook 7H9 medium is formulated with ~6 μM $CuSO_4$, we next tested 8HQ in 7H9 medium made without $CuSO_4$. Here, 8HQ was completely inactive against *M. tuberculosis* H37Rv (Fig. 1B). The addition of 6 μM $CuSO_4$ to the medium fully restored 8HQ's activity (Fig. 1B), while the addition of $CuSO_4$ to commercial Middlebrook 7H9 medium had no major impact (Fig. 1A). To exclude the possibility of medium-specific effects and to determine the full extent of the synergy between Cu and 8HQ, we repeated the experiment in Hartmans-de Bont minimal medium (HdB_{SM}), which permits the growth of *M. tuberculosis* in the absence of potentially interfering albumin supplements. Albumin is known to bind Cu and other metal ions and may therefore reduce the sensitivity of the assay (35, 45). As expected, the Cu dependency was much more pronounced, yielding an MIC of ~0.16 μM for *M. tuberculosis* H37Rv (Fig. 1C) and its avirulent surrogate, *M. tuberculosis* mc^{2}6230 (H37Rv Δ*RD1* Δ*panCD*) (Fig. 1D).

Numerous derivatives of 8HQ are marketed for a variety of antimicrobial applications in industry and medicine, including the antiprotozoal/antifungal clioquinol (CQ; see Fig. S1B in the

supplemental material) and the antibacterial nitroxoline (NQ; see Fig. S1C in the supplemental material). We found that both CQ and NQ displayed Cu-dependent activity against *M. tuberculosis* mc^{2}6230 (Fig. 1E and F), similar to 8HQ. However, in direct contrast to 8HQ and CQ, NQ actually lost its activity at concentrations above 1.25 μM in the presence of Cu ions (Fig. 1F). Spotting of samples from the NQ assays on agar plates directly confirmed the bactericidal action of NQ at lower NQ concentrations and the presence of viable cells at higher NQ concentrations (see Fig. S2 in the supplemental material).

Differences in the killing kinetics of 8HQ and NQ were also observed. While 8HQ at 0.63 μM killed *M. tuberculosis* mc^{2}6230 within 5 h of exposure in the presence of Cu ions (see Fig. S3A in the supplemental material), NQ acted much slower under comparable conditions, requiring an exposure time of ~42 h to kill *M. tuberculosis* mc^{2}6230 (see Fig. S3B in the supplemental material). We therefore suspect that the failure of NQ to kill *M. tuberculosis* mc^{2}6230 at higher concentrations may be related to Cu-mediated precipitation of the compound. Indeed, we noticed precipitation to occur at higher concentrations (>50 μM) (data not shown) upon mixing of NQ with Cu ions in test tubes, but precipitation was also observed for 8HQ and CQ under similar conditions. Given the fast-acting properties of 8HQ, we assume that 8HQ might act before precipitating out, while the potency of NQ may be more prone to precipitation due to its much slower action.

We further investigated the possible interaction between Cu ions and 8-hydroxyquinoline-2-carboxylic acid (HCA) (see Fig. S1D in the supplemental material). HCA was previously reported to inhibit the zinc-dependent fructose 1,6-bisphosphate aldolase of *M. tuberculosis* in enzymatic assays (9, 46). In accordance with previous reports (9), we confirmed that the compound is a relatively poor inhibitor of whole cells (see Fig. S4A in the supplemental material), with 500 to 1,000 μM HCA being needed to inhibit *M. tuberculosis* mc^{2}6230. In stark contrast to the findings for the other three analogs examined (Fig. 1), there was no increase in activity upon the addition of Cu (see Fig. S4A in the supplemental material). Instead, HCA reversed the toxicity of Cu ions: while 30 μM Cu inhibited *M. tuberculosis* in HdB_{SM}, addition of HCA corresponding to 2-fold or more the concentration of added Cu (e.g., ≥60 μM HCA and 30 μM Cu, ≥120 μM HCA and 60 μM Cu) caused the dose-response curve to mirror that obtained with HCA alone (see Fig. S4A in the supplemental material). Dose matrix studies using Zn in combination with HCA showed neither an enhancement nor a reduction in HCA's potency (see Fig. S4B in the supplemental material). Together, the results of these experiments indicate that the presence of Cu ions can have greatly varied effects modulating the activity of 8-hydroxyquinolines. While the activity of 8HQ, CQ, or NQ was enhanced, HCA's low-level activity remained unchanged. In addition, HCA acted as a Cu ion toxicity-averting agent.

Antibacterial properties of 8-hydroxyquinolines in combination with other metal ions. Many simple 8-hydroxyquinolines act as typical bidentate metal chelators (47–49). These complexes share nearly identical structures and geometries (see Fig. S1E and F in the supplemental material), regardless of the metal ion included. Given the complexity of the cellular milieu, 8HQ would likely encounter metals such as manganese, iron, and zinc. Due to the roles of the last two metals within the context of nutritional immunity, the viability of a Cu-dependent therapeutic rests upon whether its interaction with such metals modulates activity toward *M. tuberculosis*. Though Cu-free HdB_{SM} already contains Zn, Fe, and Mn (the recipe is detailed in Materials and Methods), we established baseline 8HQ dose-response curves by supplementing HdB_{SM} with an additional 7.5 μM $FeCl_2$, $MnCl_2$, $ZnCl_2$, or $CuCl_2$. While Cu was by far the most potent metal (MIC, 0.15 μM), Zn showed some efficacy in the presence of 10 μM 8HQ (Fig. 2A). Fe and Mn showed only a negligible inhibition at the highest 8HQ concentration tested (Fig. 2A). Similarly, CQ was the most potent in the presence of Cu, though the boost provided by Zn was much more pronounced than that for 8HQ (Fig. 2A and B). No boosting by a metal ion other than Cu was observed for NQ (Fig. 2C). HCA displayed no detectable metal-related activity on whole cells over the concentration range tested, despite being previously shown to inhibit Zn-dependent enzymes (50% inhibitory concentration, 10 μM) (9).

With the Cu specificity of 8HQ firmly established, we next sought to determine whether the presence of other metals in excess could ablate activity. After first confirming that Fe, Zn, and Mn are not toxic to *M. tuberculosis* mc^{2}6230 in HdB_{SM} up to a concentration of 1 mM (see Fig. S5A in the supplemental material), we tested 8HQ in the presence of 7.5 μM Cu and combinations of physiological levels of Fe, Zn, and/or Mn (at 20 μM each) (50) (see Fig. S5B in the supplemental material). Even in the presence of all three other metals (for a combined excess of 60 μM), 8HQ retained full Cu-dependent activity.

The copper-monoligand complexes are likely the active form of 8-hydroxyquinlines in solution. As the unique nature of inhibition is seemingly reliant on the interaction of both ligand and metal, we next investigated the identity of the active complex. 8-Hydroxyquinolones are known to coordinate Cu, as well as other bivalent metal ions, in two possible stoichiometries: either in a 1:1 ligand-ion complex (ML) (reaction I) or a 2:1 ligand-ion complex (ML_2) (reaction II). For most bivalent transition metal ions, including Cu, complex formation with 8HQ, CQ, or NQ involves two consecutive reactions: the formation of ML (reaction I) and the subsequent formation of the ML_2 complex, where a second free ligand molecule binds to the ML complex (reaction II) (see Fig. S1E and F in the supplemental material). The partial formation constants k_1 (equation 1) and k_1 (equation 2), which give rise to an overall formation constant, K_f (equation 3), characterize reactions I and II, respectively. Depending on the assay conditions, K_f values for the reaction between 8HQ and Cu or Zn vary greatly throughout the literature (see Table S1 in the supplemental material). To provide a comparable set of binding constants for the compounds investigated here, we determined k_1 and k_2 values for Cu and Zn coordination in a system buffered to pH 7.4 with relevance to our assays (see Table S2 in the supplemental material). We included Zn because it is the most abundant physiological transition metal ion and therefore Cu's most likely competitor. The experimentally determined K_f values for 8HQ and CQ complexes were in good agreement with those determined by Ferrada et al. (51), who used conditions relatable to ours (see Table S1 in the supplemental material). By using these constants and the actual input concentrations of Cu ions and ligand, we were able to project the mole fractions of free ligands (L) and both metal complexes, ML and ML_2 (see Fig. S6A in the supplemental material). These calculations suggest that at the MICs of 8HQ, CQ, and NQ (~0.16 μM), ligands are either free (L) or engaged in a 1:1 complex (ML), with nearly no 1:2 complex (ML_2) forming (see Fig. S6A in the supplemental material). The formation of the Zn com-

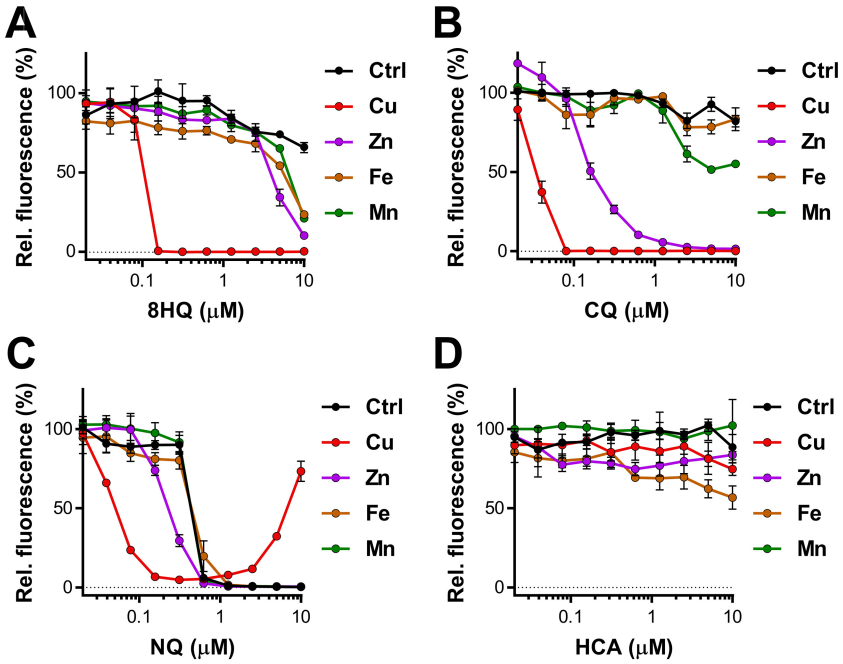

FIG 2 Metal specificity of 8-hydroxyquinolines' anti-*M. tuberculosis* activity. The anti-*M. tuberculosis* activities of 8-hydroxyquinoline (A), CQ (B), NQ (C), and HCA (D) with metal were evaluated in HdB_{SM} supplemented with 7.5 μM chloride salts of Fe, Mn, Zn, and Cu. The data shown are representative of those from at least two independently conducted experiments. Individual data points represent the means from three replicates from the same assay plate. Error bars indicate standard deviations. Background values were subtracted from all values, and all values were normalized to those for the untreated controls (Ctrl).

plexes follows a similar pattern (see Fig. S6B in the supplemental material). Mole fraction calculations using binding constants for 8HQ with other metals (Zn, Fe, Mn) from another study (12) also predict that the 1:1 complexes form (see Fig. S6C in the supplemental material). However, these binding constants represent only a very narrow snapshot of what is happening when the compounds and the metals are mixed. The equilibrium in the actual assay is expected to be highly dynamic, given the complexity of the utilized growth medium (HdB or 7H9 medium). Furthermore, mycobacterial cells might extract the ML complexes from the medium, thereby potentially driving the equilibrium toward the continuous formation of ML. This would explain why CQ is still active, even though very little of it (<1%) is predicted to convert into the 1:1 complex (see Fig. S6A in the supplemental material). Because the ligands are not active in the absence of Cu and because the 1:2 complex is unlikely to form or would likely precipitate out (12), we attribute the Cu-dependent anti-*M. tuberculosis* effects of 8-hydroxyquinolines to their 1:1 complexes.

The copper complexes of 8HQ and CQ utilize different pathways to cross the mycobacterial OM. After elucidating the 1:1 ligand-Cu complex to be the likely active component, we next examined the pathway by which 8-hydroxyquinolines likely cross the mycobacterial outer membrane (OM), which constitutes the most important permeability barrier of the mycobacterial cell envelope (52). Two passive uptake pathways are typically considered: (i) the hydrophobic pathway, by which lipophilic molecules directly penetrate the lipid layers, or (ii) the hydrophilic pathway, by which small and hydrophilic molecules utilize outer membrane channel proteins called porins for crossing (53). As it is largely unknown how *M. tuberculosis* functionalizes its OM for the uptake of molecules, we used the model organisms *M. smegmatis* SMR5 and its well-characterized triple porin mutant ML16 (Δ*mspA* Δ*mspC* Δ*mspD*) to distinguish between hydrophilic and hydrophobic uptake pathways (52). The principal outer membrane architecture of *M. smegmatis* is similar to that of *M. tuberculosis* (52, 54), and the lack of porin channels in ML16 mimics the low OM permeability of *M. tuberculosis* and mediates high-level resistance to small and hydrophilic antibiotics (e.g., β-lactam antibiotics) (52). Conversely, the lack of differences in sensitivity to a particular compound between ML16 and its wild-type strain, *M. smegmatis* SMR5, indicate that these compounds may freely cross the mycobacterial OM (52). The ML16 system is therefore ideally suited to investigate by which pathway the antibacterial copper complexes of 8HQs cross the OM. We first confirmed that 8HQ and CQ displayed Cu-dependent antibacterial properties against *M. smegmatis* SMR5 (Fig. 3A and B, respectively). Although the MICs for both compounds in the presence of Cu (1.25 μM) were ~8-fold higher than those for *M. tuberculosis* (0.16 μM) (Fig. 1), the micromolar sensitivity validates *M. smegmatis* as a suitable model to assess how the copper complexes of 8HQ and CQ enter mycobacterial cells. Unfortunately, NQ displayed only Cu-independent activity against *M. smegmatis* (Fig. 3C), precluding us from investigating its copper-dependent activity in this model. We found that ML16 was more resistant to CQ than the wild-type strain (SMR5) or its MspA-complemented counterpart (Fig. 3B). In analogy to ML16's increased resistance to small and hydrophilic antibiotics (52), the CQ data suggest that the CQ-Cu complex is unable to freely cross the mycobacterial OM. In stark contrast, the lack of porins in the OM of *M. smegmatis* ML16 did not significantly alter the activity of 8HQ in the presence of Cu, which is indicative of direct penetration across the OM (Fig. 3A). Together, these data suggest that the minor structural differences

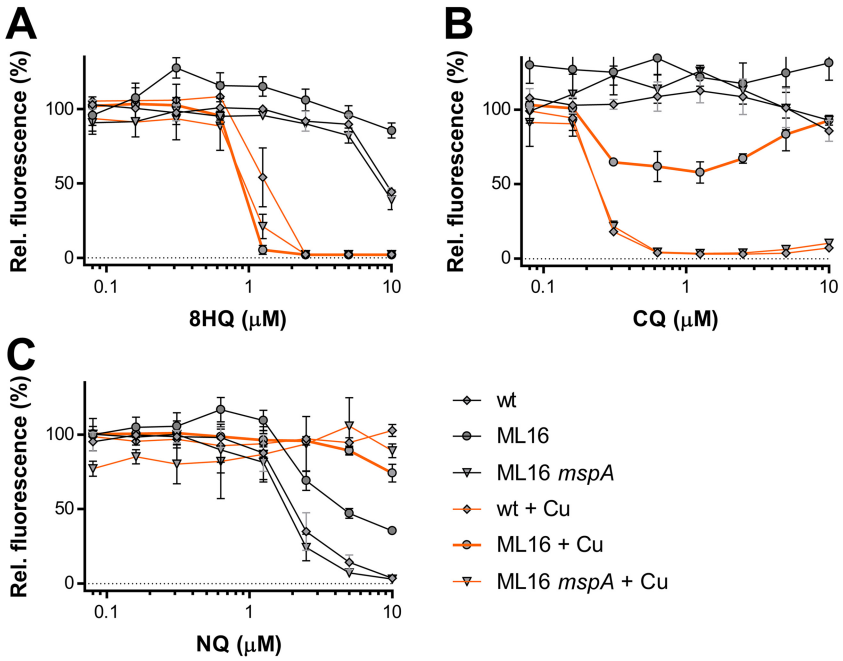

FIG 3 Impact of MspA-mediated outer membrane permeability on the activity of 8HQs against *M. smegmatis* SMR5. Dose-response curves of the *M. smegmatis* wild type (wt), its triple porin mutant ML16, and the MspA-expressing ML16 strain (ML16 *mspA*) against 8-hydroxyquinoline (A), CQ (B), and NQ (C) in the presence or absence of $CuSO_4$. Error bars represent standard deviations from at least three sample replicates. Individual data points represent the means from three replicates from the same assay plate. Error bars indicate standard deviations. Background values were subtracted from all values, and all values were normalized to those for the untreated controls.

between 8HQ and CQ, which is only two atoms (see Fig. S1A and B in the supplemental material) impact the mechanism by which these compounds cross the mycobacterial OM.

Cotreatment with 8HQ and copper leads to an increase in the amount of the cell-associated labile metal pool. As a class, Cu-dependent inhibitors are known to act through a wide range of mechanisms. They can act as ionophores, overloading cells with Cu ions (e.g., 8HQ against *Cryptococcus neoformans* [28]); as liberators, growing the pool of bioavailable (and toxic) Cu without an overall increase (e.g., disulfiram against *M. tuberculosis* [45]); and even as traditional antibiotics, disrupting specific enzymatic targets (e.g., glyoxal-bis[N(4)-methylthiosemicarbazonato]copper(II) complex against *Neisseria gonorrhoeae* [55]). To gain insight into the mechanism of mycobacterial inhibition, we utilized PhenGreen FL (PGFL), a fluorescent metal sensor, to determine net changes in the amounts of cell-associated labile metal ions upon treatment with Cu or 8HQ alone or cotreatment with Cu ions and 8HQ. Because PGFL requires metabolic activation upon entry into cells, the assay can be performed only on viable cells. As we already determined that 8HQ-Cu treatment kills *M. tuberculosis* mc^{2}6230 within 5 h of exposure (see Fig. S3A in the supplemental material), we opted for a 2-h treatment period, which did not affect viability (see Fig. S7A in the supplemental material). We chose to compare 8HQ and HCA due to their contrasting activity profiles in the presence of copper (Fig. 2A and D). As the Cu content is the only metal-related variable that changed in our experiments, we attribute the quenching of fluorescence to an upshift of the cell-associated labile Cu ion content. In comparison to the results for the untreated control, the treatments with 2.5 μM Cu or 0.62 μM 8HQ alone did not affect PGFL fluorescence (Fig. 4A). As expected, treatment with 50 μM Cu dramatically reduced the fluorescence (Fig. 4B). Interestingly, cotreatment of *M. tuberculosis* mc^{2}6230 with 8HQ in the presence of 2.5 μM Cu then showed a 76% reduction in fluorescence (Fig. 4A). In stark contrast, cotreatment of cells with high concentrations of Cu (50 μM) and HCA (100 μM) counteracted the quenching, despite the high Cu ion content (Fig. 4B). The observed lack of quenching in the presence of 50 μM Cu is consistent with HCA's ability to avert Cu ion toxicity at high concentrations (see Fig. S4A in the supplemental material), likely by preventing Cu from accumulating inside the cells. Conversely, the ability of 8HQ to quench PGFL fluorescence in the presence of low Cu concentrations suggests that 8HQ acts as a Cu ionophore facilitating the accumulation of bioavailable Cu ions inside the cell.

In the presence of copper, 8HQ is as effective against *M. tuberculosis* mc^{2}6230 cells recovering from starvation as their replicating counterparts. A major challenge in antituberculosis therapeutics is that of dormant, nonreplicating *M. tuberculosis* cells. These bacteria are phenotypically drug resistant, necessitating lengthy treatment regimens (56). To control the disease, it is vital to target this population both to prevent the subsequent reactivation of latent *M. tuberculosis* and to avoid the generation of drug-resistant strains (57). To determine the efficacy of 8HQ against dormant populations, nonreplicating cells were generated using the standard *M. tuberculosis* starvation protocol (36). These nonreplicating cells were then transferred into $7H9_{SM}$ for treatment and assessed for their ability to recover/survive in the presence of 8HQ with or without 7.5 μM Cu. We chose to investigate only 8HQ, as it showed the highest degree of Cu specificity and a lack of Cu-independent activity in prior assays (Fig. 2). The MIC of 8HQ in the presence of Cu ions for cells recovering from starvation was similar to the one obtained for replicating cells receiving an iden-

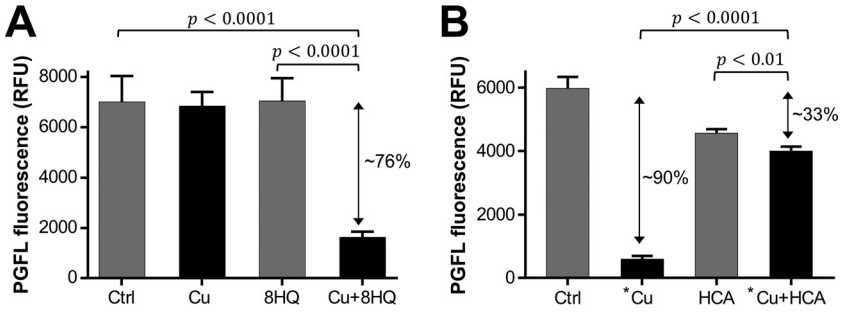

FIG 4 The contrasting effects of 8HQ and HCA on the cell-associated labile copper pool of *M. tuberculosis* mc^{2}6230. Cells were treated with 2.5 μM copper (Cu) or 0.62 μM 8HQ alone or in combination (A) or were treated with 50 μM copper (*Cu) or 100 μM HCA alone or in combination (B). Untreated controls (Ctrl) were included in both assays. A Student's *t*-test (two-tailed) was performed to evaluate the significance of the difference between fluorescence intensities detected from the indicated conditions. *P* values are given in the graphs. The data sets are representative of those from at least two independent experiments, and the error bars indicate the standard errors from three technical replicates. Double-headed arrows, reduction of fluorescence relative to that for the untreated control; RFU, relative fluorescence units.

tical treatment (1.25 μM). Interestingly, cells recovering from starvation even showed sensitivity to 8HQ in the absence of Cu ions (Fig. 5A), which we did not observe for replicating cells (Fig. 5A and 1B). The MIC of 8HQ for latent cells in the presence of Cu ions is in good agreement with the MIC previously determined by other investigators (~3.3 μM) in commercial Middlebrook medium (8). Additionally, spotting of samples from each well on 7H10 agar plates confirmed that both cells recovering from starvation and replicating cells were killed at the respective MICs (Fig. 5B). The Cu-independent mode of action on recovering cells suggests that 8HQ may act by multiple mechanisms dependent on the metabolic state of the cells.

Toxicity and antibacterial effects of 8HQ on *M. tuberculosis* mc^{2}6230-infected primary macrophages. Finally, we wanted to examine whether the Cu-dependent nature of inhibition could be harnessed in a pseudo-*in vivo* model of macrophage infection. For this, we focused our investigation on 8HQ because its activity displayed the highest degree of Cu specificity in the absence of Cu-independent inhibition (Fig. 2). 8HQ was nontoxic in standard medium (RPMI 1640 medium plus 10% FBS), as determined by means of bright-field microscopy (see Fig. S8 in the supplemental material) with the metabolic cell health indicator dye resazurin (Fig. 6A). We treated *M. tuberculosis* mc^{2}6230-infected peritoneal macrophages with 8HQ and determined the number of viable intracellular bacteria (CFU counts) (Fig. 6B). In comparison to the results for the untreated control, the number of CFU in

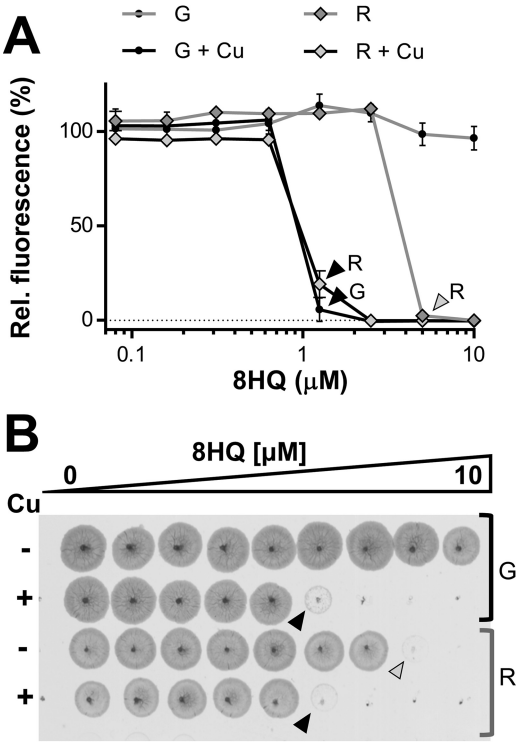

FIG 5 Activity of 8HQ on *M. tuberculosis* mc^{2}6230 cells recovering from starvation in 7H9$_{SM}$ under growth permissive conditions. (A) Dose-response profile of 8HQ on growing (G) and recovering (R) cells in the presence or absence of 7.5 μM $CuSO_4$. Individual data points represent the means from three replicates from the same assay plate. Error bars indicate standard deviations. Background values were subtracted from all values, and all values were normalized to those for the untreated controls. (B) Samples (5 μl) from the actual dose-response assay plate were spotted on 7H10 agar to confirm the results obtained from the dose-response curve shown in panel A. Black and gray arrowheads, MICs in the presence (+) and absence (−) of 7.5 μM $CuSO_4$ (Cu), respectively. The concentration differential of 8HQ between individual data points is 2-fold, with the maximum being 10 μM.

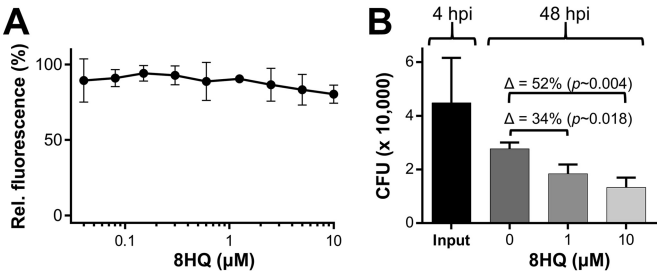

FIG 6 Efficacy of 8HQ against intracellular *M. tuberculosis* mc^{2}6230. (A) Sensitivity of peritoneal murine macrophages to 8HQ in standard cell culture medium (RPMI 1640 medium) supplemented with 10% heat-inactivated fetal bovine serum. (B) *M. tuberculosis* mc^{2}6230-infected macrophages were treated for 48 h with 1 or 10 μM 8HQ (as indicated on the *x* axis). Upon completion of treatment, macrophages were lysed, and serial dilutions of the lysate were plated on 7H10 agar for determination of CFU counts. The data are representative of those from two independent experiments with similar outcomes. Data points represent the averages for three identically treated wells, with the standard deviations being shown. Δ, change in the numbers of CFU; hpi, hours postinfection.

1 and 10 μM 8HQ-treated samples was reduced by ~34% and ~52%, respectively. Given that 8HQ is unable to kill *M. tuberculosis* in the absence of Cu (Fig. 1), we conclude that intracellular *M. tuberculosis* mc^{2}6230 is exposed to the 8HQ-Cu complex. To determine whether 8HQ utilizes Cu from the cell culture medium, we treated *M. tuberculosis* mc^{2}6230 with 8HQ in RPMI 1640 medium and performed a fluorescein diacetate viability stain on *M. tuberculosis* cells 48 h later. Flow cytometry detected high fluorescence (see Fig. S9 in the supplemental material) in these cells, suggesting that the Cu ion content in RPMI 1640 medium is not sufficient to activate the antibacterial properties of 8HQ. In contrast, no fluorescence was detected in *M. tuberculosis* cells cotreated with 8HQ and Cu in HdB_{SM} (see Fig. S9 in the supplemental material), which was to be expected, given the already established bactericidal action of 8HQ under those conditions (see Fig. S3 in the supplemental material). As the Cu ions in RPMI 1650 medium (1 to 2 μM Cu stems from the addition of 10% FBS) are sequestered by serum proteins (e.g., albumin, ceruloplasmin) and we already observed a decreased potency of 8HQ in albumin-containing 7H9 medium (Fig. 1), we conclude that the Cu ion content of RPMI 1640 medium is insufficient for 8HQ to become bactericidal. Therefore, our data suggest that 8HQ acquires Cu ions inside the macrophage, perhaps taking advantage of the native Cu ion pool within *M. tuberculosis*-containing phagosomes, whose concentration peaks at 400 μM (17).

DISCUSSION

The metal-binding abilities of 8HQ and its derivatives are well established and in many, though not all, cases have been linked to their anticancer, neuroprotective, and antimicrobial activity (2). One notable exception is mycobacteria (2, 8), against which 8HQ's Cu requirement for activity remained unobserved in previous studies (7, 8). In this study, we were able to clearly demonstrate that in these previous experiments the Cu ion content of commercial Middlebrook 7H9 medium disguised the Cu ion dependency of 8HQ (Fig. 1). The only existing experimental evidence for a metal-related mode of action for this type of compound against *M. tuberculosis* therefore probably comes from *in vitro* enzymatic screens on mycobacterial metalloenzymes. The most recent targets were the two methionine aminopeptidases *metA* (*rv0734*) and *metB* (*rv2861c*) and fructose 1,6-bisphosphate aldolase (*fba*, *rv0363c*) (9, 46, 58). These enzymes are inhibited by the 8HQ derivative HCA through documented interactions between the inhibitor and a catalytically essential zinc or cobalt ion (9, 46, 58). However, an often observed shortcoming of enzymatic inhibitors from such target-based approaches is the lack of significant activity on respective model organisms (59), and unfortunately, HCA is no exception (9). The failure of HCA to effectively inhibit the growth of *M. tuberculosis* in culture medium (see Fig. S4 in the supplemental material) (9) suggests either that the enzyme in its natural environment is inaccessible to the inhibitor or that any enzymatic inhibition that does occur is not significant enough to produce relevant phenotypic inhibition. The high MIC of HCA (500 μM) may suggest that its ability to bind trace metal ions may simply deprive cells of these essential nutrients. This is particularly likely when, as in the case of HCA, the chelator concentration exceeds the combined transition metal ion content of the medium (in HdB medium, the Zn, Fe, Mn, and Co ion concentration combined is 35 μM) or, as recently reported for a novel pyrazolopyrimidinone, when the molecule acts as an intracellular metal chelator (60). The Cu ion toxicity-averting action for HCA observed here (see Fig. S4A in the supplemental material) would then suggest that Cu chelation by HCA reduces Cu's bioavailability and, thereby, its toxic impact on *M. tuberculosis*.

In stark contrast to the findings for HCA, the combination of 8HQ and Cu ions manifests a growth-inhibitory phenotype on *M. tuberculosis* at concentrations of Cu ions or 8HQ that are nontoxic to *M. tuberculosis* when each one is administered individually (Fig. 1). Given the well-characterized coordination chemistry of 8HQ, it is straightforward to anticipate that this antibacterial action is related to the formation of an 8HQ-Cu complex. Such Cu complexes have been described for all 8-hydroxyquinolines investigated herein (28, 61, 62). However, the identity of the complex endowed with said activity is uncertain. 8HQ can form Cu complexes of a 1:1 or 1:2 metal/ligand ratio (see Fig. S1E and F, respectively, in the supplemental material). This process depends on the concentration of Cu relative to that of the ligand (12). On the basis of the very poor solubility of the 1:2 complex (63), available formation constants (see Tables S1 and S2 in the supplemental material), and actual concentration ratios in our system, it is unlikely that the observed Cu-dependent activity of 8HQ depends on the formation of a 1:2 complex. As our calculations indicate that only the 1:1 complex forms in our assays (see Fig. S6A in the supplemental material), we attribute the Cu-related anti-*M. tuberculosis* activity of 8HQ to the formation of the 1:1 complex.

Given that the 1:1 complex carries a positive net charge, we next investigated potential pathways by which the 1:1 complex enters the mycobacterial cell. Charged molecules are typically not expected to simply diffuse freely through membranes. Thus, mycobacterial porins may provide a possible entry pathway, at least across the outer membrane. However, our data only vaguely indicate that the CQ-Cu complex may utilize porins to enter the cell. The activity of 8HQ-Cu was porin independent in *M. smegmatis* (Fig. 5), pointing toward the possibility that the active form of 8HQ can freely cross the mycobacterial OM. While our investigations are inevitably limited to MspA, which is currently the only mycobacterial porin known to facilitate the passage of small and hydrophilic molecules (including antibiotics) across the mycobacterial OM (52, 64, 65), we cannot exclude the possible involvement of yet unidentified porins or other factors that may facilitate the uptake of 8HQ-Cu complexes, particularly in the context of *M. tuberculosis*.

Alternatively, one could also hypothesize an association of the 1:1 complex with one or more additional ligands. This may neutralize the net charge of the resulting mixed ligand complex. Double-positive Cu ions favor octahedral, square planar, or tetrahedral coordination geometries (66). It is therefore important to note that the 8HQ-Cu complex is likely associated with other neutral or anionic medium constituents (e.g., H_2O, Cl^-, or OH^-) to accommodate the coordination geometries of Cu. In a highly dynamic manner, this process may generate a variety of neutral mixed ligand complexes able to cross the mycobacterial OM. Other potential ligand candidates could be free amino acids or citrate, which are also able to coordinate copper with a reasonable affinity. These components were present in our medium, and antibacterial synthetic mixed ligand complexes of 8HQ-Cu and various amino acids or citrate have been reported previously (67, 68).

Another interesting aspect is the lack of 8HQ's antimycobacterial properties in the absence of Cu and the presence of other bivalent transition metal ions. If one considers the Irving-Wil-

liams series of relative metal complex stabilities (14), one could hypothesize that the affinity of the 8HQ scaffold for Cu ions may be a determining factor. Indeed, the series typically identifies Cu to be the physiologically relevant transition metal ion with the highest affinity for many simple-structured metal-binding ligands. This correlation also applies to 8HQ (12) and was confirmed at least for Cu and Zn ions in our system (see Table S2 in the supplemental material). The significantly weaker effects of other metal ions or the complete lack thereof (Fig. 2A) may therefore partially reflect this correlation. However, under consideration of published K_f values (12) and the concentrations given in our system, the impact of 8HQ's affinity for a particular metal ion (Zn, Fe, or Mn) appears to be negligible. Any of the respective 1:1 metal complexes are expected to form (see Fig. S5C in the supplemental material). The activity is therefore more likely related to the intrinsic properties of the associated metal ion (e.g., antibacterial activity), with the ligand being responsible for the disguise and delivery of the proper metal ion to a sensitive target site. The entire complex could then resemble a Trojan horse, as previously proposed by us in the context of the Cu-active drug disulfiram (45). In such a scenario, the complex would be expected to act on targets within the cell. These targets are still unknown, but their identification is a current focus in our laboratories.

Lastly, we tested 8HQ for efficacy against intracellular *M. tuberculosis* in a primary macrophage infection model. In similarity with a study by Festa et al. (28), who investigated the efficacy of 8HQ against *Cryptococcus neoformans*-infected macrophages and mice, we, too, found 8HQ to be effective in killing intracellular microbes. Given the strict Cu-dependent nature of 8HQ's activity against both *M. tuberculosis* and the pathogenic fungus *C. neoformans*, these data collectively suggest that 8HQ's action against intracellular microbes may be linked and dependent upon host cell-derived intracellular Cu ion pools. We exclude the possibility that 8HQ would deplete Cu ions from essential intracellular Cu ion reservoirs (e.g., mitochondrial respiration), as this would likely kill the host cell, which we did not observe (Fig. 6A; see also Fig. S8 in the supplemental material). Besides, while we determined an affinity of 8HQ for Cu in the nanomolar range ($\log K_f = 9.22$; see Table S2 in the supplemental material), intracellular Cu-requiring proteins bind Cu ions with much greater affinities (69, 70). These protein-bound Cu ions are therefore unlikely accessible to 8HQ. In addition, free Cu ions do not exist within the cytoplasm of any cell (71). Therefore, 8HQ would most likely associate with other transition metal ions, such as Zn, Fe, or Mn, which are considerably more abundant than Cu and less tightly bound to proteins (72). However, as these metal ions do not bestow significant activity to 8HQ, the presence of other, more easily accessible intracellular Cu pools must be considered. Previous reports established the presence of Cu ions in macrophage phagosomes in response to microbial encounters (16, 17). In the absence of any known phagosomal Cu-binding or sequestration proteins, phagosomal Cu ions would be expected to be thermodynamically less restricted than its protein-incorporated counterparts. It is therefore straightforward to propose that the phagosomal Cu ion content may render 8HQ active against bacteria, at least inside the phagosome. Hence, our data (Fig. 6) suggest a possible link between Cu-related innate immunity and the efficacy of antibiotics with Cu-dependent activities. Our data, however, do not exclude the possibility that the antibacterial properties of 8HQ in the macrophage model may be due to potential interactions with or activation of Cu-independent antibacterial host responses.

In conclusion, our data illustrate that the interaction of metals with chelating drugs can impart a broad spectrum of antibacterial activities to the complex that is formed. We observed activity gain or loss (e.g., for 8HQ versus NQ on *M. smegmatis*; Fig. 3A and C), metal specificity or promiscuity (e.g., for 8HQ versus CQ; Fig. 2A and B), porin dependency or independency in *M. smegmatis* (for 8HQ versus CQ; Fig. 3A and B), the entire spectrum of metal-dependent or -independent activities (for 8HQ versus NQ versus HCA; Fig. 1; see also Fig. S4A in the supplemental material), and, finally, enhancement or aversion of Cu-related toxicity (for 8HQ versus HCA; Fig. 1D; see also Fig. S4A in the supplemental material). Therefore, generalizations regarding activity/toxicity even between metal chelates of closely related ligands or projections toward the properties of unrelated metal-binding scaffolds should be made with caution. On the other hand, this spectrum of metal-related activities, along with the structural simplicity and chemical accessibility of 8-hydroxyquinoline, establish the 8-hydroxyquinoline scaffold to be an ideal structural cluster for in-depth studies elucidating structure-activity relationships on metal-binding preferences, membrane permeability, and antibacterial activity. Such systematic studies would lay the foundation for the structure-based development and analysis of the medicinal chemistry of 8-hydroxyquinolines focusing on metal-related aspects of their antibacterial properties in conjunction with metal-related innate immunity.

ACKNOWLEDGMENTS

We thank Saran Kupul for her excellent technical assistance and lab management. We are also grateful to Bill Jacobs for providing *M. tuberculosis* $mc^2$6230 and Michael Niederweis for providing the *M. smegmatis* porin mutant ML16 and the plasmid pMN016.

This study was supported by National Institutes of Health (NIH) grant R01 AI104952 to F.W. and funds from the National Science Foundation (DMR number 1242765) awarded to S.H.B.

FUNDING INFORMATION

This work, including the efforts of Frank Wolschendorf, Santosh Shah, and Alex G. Dalecki, was funded by HHS | NIH | National Institute of Allergy and Infectious Diseases (NIAID) (R01 AI104952). This work, including the efforts of Stefan H. Bossmann, was funded by National Science Foundation (NSF) (1242785).

A portion of this study was supported in part by the University of Alabama at Birmingham's (UAB) Center for AIDS Research (CFAR) and its Cytometry Core/Joint UAB Flow Cytometry Core, which are funded by NIH/NIAID P30 AI027767 and by NIH 5P30 AR048311. The funders had no role in study design, data collection and interpretation, or the decision to submit the work for publication.

REFERENCES

1. **World Health Organization.** 2015. Global tuberculosis report 2015. World Health Organization, Geneva, Switzerland.
2. **Song Y, Xu H, Chen W, Zhan P, Liu X.** 2015. 8-Hydroxyquinoline: a privileged structure with a broad-ranging pharmacological potential. MedChemComm **6:**61–74. http://dx.doi.org/10.1039/C4MD00284A.
3. **Hongmanee P, Rukseree K, Buabut B, Somsri B, Palittapongarnpim P.** 2007. *In vitro* activities of cloxyquin (5-chloroquinolin-8-ol) against *Mycobacterium tuberculosis*. Antimicrob Agents Chemother **51:**1105–1106. http://dx.doi.org/10.1128/AAC.01310-06.
4. **Urbanski T, Slopek S, Venulet J.** 1951. Antitubercular activity of some 8-hydroxyquinoline derivatives. Nature **168:**29. http://dx.doi.org/10.1038/168029a0.

5. **Tison F.** 1952. The remarkable effect of a combination of iodochloroxyquinoline with a subactive dose of streptomycin on experimental tuberculosis in guinea pigs. Ann Inst Pasteur (Paris) **83:**275–276. (In French.)
6. **McElroy J.** 1910. The treatment of pulmonary tuberculosis by intravenous injections of chinosol with formaldehyde. Lancet **176:**1408–1409. http://dx.doi.org/10.1016/S0140-6736(01)08447-1.
7. **Ananthan S, Faaleolea ER, Goldman RC, Hobrath JV, Kwong CD, Laughon BE, Maddry JA, Mehta A, Rasmussen L, Reynolds RC, Secrist JA, III, Shindo N, Showe DN, Sosa MI, Suling WJ, White EL.** 2009. High-throughput screening for inhibitors of *Mycobacterium tuberculosis* H37Rv. Tuberculosis (Edinb) **89:**334–353. http://dx.doi.org/10.1016/j.tube.2009.05.008.
8. **Darby CM, Nathan CF.** 2010. Killing of non-replicating *Mycobacterium tuberculosis* by 8-hydroxyquinoline. J Antimicrob Chemother **65:**1424–1427. http://dx.doi.org/10.1093/jac/dkq145.
9. **Capodagli GC, Sedhom WG, Jackson M, Ahrendt KA, Pegan SD.** 2014. A noncompetitive inhibitor for *Mycobacterium tuberculosis*'s class IIa fructose 1,6-bisphosphate aldolase. Biochemistry **53:**202–213. http://dx.doi.org/10.1021/bi401022b.
10. **Rubbo SD, Albert A, Gibson MI.** 1950. The influence of chemical constitution on antibacterial activity. V. The antibacterial action of 8-hydroxyquinoline (oxine). Br J Exp Pathol **31:**425–441.
11. **Albert A, Rubro SD.** 1947. The influence of chemical constitution of antibacterial activity; a study of 8-hydroxyquinolin (oxine) and related compounds. Br J Exp Pathol **28:**69–87.
12. **Albert A, Gibson MI, Rubbo SD.** 1953. The influence of chemical constitution on antibacterial activity. VI. The bactericidal action of 8-hydroxyquinoline (oxine). Br J Exp Pathol **34:**119–130.
13. **Albert A, Hampton A, Selbie FR, Simon RD.** 1954. The influence of chemical constitution on anti-bacterial activity. VII. The site of action of 8-hydroxy-quinoline (oxine). Br J Exp Pathol **35:**75–84.
14. **Irving H, Williams RJP.** 1953. 637. The stability of transition-metal complexes. J Chem Soc (Resumed) **1953:**3192–3210. http://dx.doi.org/10.1039/JR9530003192:3192-3210.
15. **Steger HF, Corsini A.** 1973. Stability of metal oxinates. I. Effect of ligand basicity. J Inorg Nucl Chem **35:**1621–1636. http://dx.doi.org/10.1016/0022-1902(73)80253-2.
16. **White C, Lee J, Kambe T, Fritsche K, Petris MJ.** 2009. A role for the ATP7A copper-transporting ATPase in macrophage bactericidal activity. J Biol Chem **284:**33949–33956. http://dx.doi.org/10.1074/jbc.M109.070201.
17. **Wagner D, Maser J, Lai B, Cai Z, Barry CE, III, Honer Zu Bentrup K, Russell DG, Bermudez LE.** 2005. Elemental analysis of *Mycobacterium avium*-, *Mycobacterium tuberculosis*-, and *Mycobacterium smegmatis*-containing phagosomes indicates pathogen-induced microenvironments within the host cell's endosomal system. J Immunol **174:**1491–1500. http://dx.doi.org/10.4049/jimmunol.174.3.1491.
18. **Wolschendorf F, Ackart D, Shrestha TB, Hascall-Dove L, Nolan S, Lamichhane G, Wang Y, Bossmann SH, Basaraba RJ, Niederweis M.** 2011. Copper resistance is essential for virulence of *Mycobacterium tuberculosis*. Proc Natl Acad Sci U S A **108:**1621–1626. http://dx.doi.org/10.1073/pnas.1009261108.
19. **Via LE, Lin PL, Ray SM, Carrillo J, Allen SS, Eum SY, Taylor K, Klein E, Manjunatha U, Gonzales J, Lee EG, Park SK, Raleigh JA, Cho SN, McMurray DN, Flynn JL, Barry CE, III.** 2008. Tuberculous granulomas are hypoxic in guinea pigs, rabbits, and nonhuman primates. Infect Immun **76:**2333–2340. http://dx.doi.org/10.1128/IAI.01515-07.
20. **Flynn JL, Chan J, Lin PL.** 2011. Macrophages and control of granulomatous inflammation in tuberculosis. Mucosal Immunol **4:**271–278. http://dx.doi.org/10.1038/mi.2011.14.
21. **Zimnicka AM, Tang H, Guo Q, Kuhr FK, Oh MJ, Wan J, Chen J, Smith KA, Fraidenburg DR, Choudhury MS, Levitan I, Machado RF, Kaplan JH, Yuan JX.** 2014. Upregulated copper transporters in hypoxia-induced pulmonary hypertension. PLoS One **9:**e90544. http://dx.doi.org/10.1371/journal.pone.0090544.
22. **White C, Kambe T, Fulcher YG, Sachdev SW, Bush AI, Fritsche K, Lee J, Quinn TP, Petris MJ.** 2009. Copper transport into the secretory pathway is regulated by oxygen in macrophages. J Cell Sci **122:**1315–1321. http://dx.doi.org/10.1242/jcs.043216.
23. **Xie L, Collins JF.** 2011. Transcriptional regulation of the Menkes copper ATPase (Atp7a) gene by hypoxia-inducible factor (HIF2a) in intestinal epithelial cells. Am J Physiol Cell Physiol **300:**C1298–C1305. http://dx.doi.org/10.1152/ajpcell.00023.2011.
24. **Graham JE, Clark-Curtiss JE.** 1999. Identification of *Mycobacterium tuberculosis* RNAs synthesized in response to phagocytosis by human macrophages by selective capture of transcribed sequences (SCOTS). Proc Natl Acad Sci U S A **96:**11554–11559. http://dx.doi.org/10.1073/pnas.96.20.11554.
25. **Talaat AM, Lyons R, Howard ST, Johnston SA.** 2004. The temporal expression profile of *Mycobacterium tuberculosis* infection in mice. Proc Natl Acad Sci U S A **101:**4602–4607. http://dx.doi.org/10.1073/pnas.0306023101.
26. **Ward SK, Abomoelak B, Hoye EA, Steinberg H, Talaat AM.** 2010. CtpV: a putative copper exporter required for full virulence of *Mycobacterium tuberculosis*. Mol Microbiol **77:**1096–1110. http://dx.doi.org/10.1111/j.1365-2958.2010.07273.x.
27. **Shi X, Festa RA, Ioerger TR, Butler-Wu S, Sacchettini JC, Darwin KH, Samanovic MI.** 2014. The copper-responsive RicR regulon contributes to *Mycobacterium tuberculosis* virulence. mBio **5:**e00876-13. http://dx.doi.org/10.1128/mBio.00876-13.
28. **Festa RA, Helsel ME, Franz KJ, Thiele DJ.** 2014. Exploiting innate immune cell activation of a copper-dependent antimicrobial agent during infection. Chem Biol **21:**977–987. http://dx.doi.org/10.1016/j.chembiol.2014.06.009.
29. **Neyrolles O, Wolschendorf F, Mitra A, Niederweis M.** 2015. Mycobacteria, metals, and the macrophage. Immunol Rev **264:**249–263. http://dx.doi.org/10.1111/imr.12265.
30. **Darwin KH.** 2015. *Mycobacterium tuberculosis* and copper: a newly appreciated defense against an old foe? J Biol Chem **290:**18962–18966. http://dx.doi.org/10.1074/jbc.R115.640193.
31. **Sander P, Meier A, Bottger EC.** 1995. rpsL$^+$: a dominant selectable marker for gene replacement in mycobacteria. Mol Microbiol **16:**991–1000. http://dx.doi.org/10.1111/j.1365-2958.1995.tb02324.x.
32. **Stephan J, Bender J, Wolschendorf F, Hoffmann C, Roth E, Mailander C, Engelhardt H, Niederweis M.** 2005. The growth rate of *Mycobacterium smegmatis* depends on sufficient porin-mediated influx of nutrients. Mol Microbiol **58:**714–730. http://dx.doi.org/10.1111/j.1365-2958.2005.04878.x.
33. **Sambandamurthy VK, Derrick SC, Hsu T, Chen B, Larsen MH, Jalapathy KV, Chen M, Kim J, Porcelli SA, Chan J, Morris SL, Jacobs WR, Jr.** 2006. *Mycobacterium tuberculosis* DRD1 DpanCD: a safe and limited replicating mutant strain that protects immunocompetent and immunocompromised mice against experimental tuberculosis. Vaccine **24:**6309–6320. http://dx.doi.org/10.1016/j.vaccine.2006.05.097.
34. **Weber FJ, van Berkel WJ, Hartmans S, de Bont JA.** 1992. Purification and properties of the NADH reductase component of alkene monooxygenase from *Mycobacterium* strain E3. J Bacteriol **174:**3275–3281.
35. **Speer A, Shrestha TB, Bossmann SH, Basaraba RJ, Harber GJ, Michalek SM, Niederweis M, Kutsch O, Wolschendorf F.** 2013. Copper-boosting compounds: a novel concept for antimycobacterial drug discovery. Antimicrob Agents Chemother **57:**1089–1091. http://dx.doi.org/10.1128/AAC.01781-12.
36. **Betts JC, Lukey PT, Robb LC, McAdam RA, Duncan K.** 2002. Evaluation of a nutrient starvation model of *Mycobacterium tuberculosis* persistence by gene and protein expression profiling. Mol Microbiol **43:**717–731. http://dx.doi.org/10.1046/j.1365-2958.2002.02779.x.
37. **Haeili M, Moore C, Davis CJC, Cochran JB, Shah S, Shrestha TB, Zhang Y, Bossmann SH, Benjamin WH, Kutsch O, Wolschendorf F.** 2014. Copper complexation screen reveals compounds with potent antibiotic properties against methicillin-resistant *Staphylococcus aureus*. Antimicrob Agents Chemother **58:**3727–3736. http://dx.doi.org/10.1128/AAC.02316-13.
38. **Norden MA, Kurzynski TA, Bownds SE, Callister SM, Schell RF.** 1995. Rapid susceptibility testing of Mycobacterium tuberculosis (H37Ra) by flow cytometry. J Clin Microbiol **33:**1231–1237.
39. **Van Deun A, Maug AK, Hossain A, Gumusboga M, de Jong BC.** 2012. Fluorescein diacetate vital staining allows earlier diagnosis of rifampicin-resistant tuberculosis. Int J Tuberc Lung Dis **16:**1174–1179. http://dx.doi.org/10.5588/ijtld.11.0166.
40. **Thordarson P.** 2012. Binding constants and their measurement. In Supramolecular chemistry: from molecules to nanomaterials. John Wiley & Sons, Ltd, Chichester, United Kingdom. http://dx.doi.org/10.1002/9780470661345.smc018.
41. **Thordarson P.** 2011. Determining association constants from titration experiments in supramolecular chemistry. Chem Soc Rev **40:**1305–1323. http://dx.doi.org/10.1039/C0CS00062K.
42. **Zhu C, Byrd RH, Lu P, Nocedal J.** 1997. Algorithm 778: L-BFGS-B: Fortran subroutines for large-scale bound-constrained optimization.

ACM Trans Math Softw **23:**550–560. http://dx.doi.org/10.1145/279232.279236.
43. **Zhang P, Katz J, Michalek SM.** 2009. Glycogen synthase kinase-3beta (GSK3beta) inhibition suppresses the inflammatory response to Francisella infection and protects against tularemia in mice. Mol Immunol **46:**677–687. http://dx.doi.org/10.1016/j.molimm.2008.08.281.
44. **Dalecki AG, Wolschendorf F.** 2016. Development of a web-based tool for automated processing and cataloging of a unique combinatorial drug screen. J Microbiol Methods **126:**30–34. http://dx.doi.org/10.1016/j.mimet.2016.04.013.
45. **Dalecki AG, Haeili M, Shah S, Speer A, Niederweis M, Kutsch O, Wolschendorf F.** 2015. Disulfiram and copper ions kill *Mycobacterium tuberculosis* in a synergistic manner. Antimicrob Agents Chemother **59:**4835–4844. http://dx.doi.org/10.1128/AAC.00692-15.
46. **Labbe G, Krismanich AP, de Groot S, Rasmusson T, Shang M, Brown MD, Dmitrienko GI, Guillemette JG.** 2012. Development of metal-chelating inhibitors for the class II fructose 1,6-bisphosphate (FBP) aldolase. J Inorg Biochem **112:**49–58. http://dx.doi.org/10.1016/j.jinorgbio.2012.02.032.
47. **Levinson W, Rohde W, Mikelens P, Jackson J, Antony A, Ramakrishnan T.** 1977. Inactivation and inhibition of Rous sarcoma virus by copper-binding ligands: thiosemicarbazones, 8-hydroxyquinolines, and isonicotinic acid hydrazide. Ann N Y Acad Sci **284:**525–532. http://dx.doi.org/10.1111/j.1749-6632.1977.tb21985.x.
48. **Weismann K.** 1986. Chelating drugs and zinc. Dan Med Bull **33:**208–211.
49. **Levinson W, Mikelens P, Jackson J.** 1977. Anti-tumor virus activity of copper-binding drugs. Adv Exp Med Biol **91:**161–178.
50. **Harrington JM, Young DJ, Essader AS, Sumner SJ, Levine KE.** 2014. Analysis of human serum and whole blood for mineral content by ICP-MS and ICP-OES: development of a mineralomics method. Biol Trace Elem Res **160:**132–142. http://dx.doi.org/10.1007/s12011-014-0033-5.
51. **Ferrada E, Arancibia V, Loeb B, Norambuena E, Olea-Azar C, Huidobro-Toro JP.** 2007. Stoichiometry and conditional stability constants of Cu(II) or Zn(II) clioquinol complexes; implications for Alzheimer's and Huntington's disease therapy. Neurotoxicology **28:**445–449. http://dx.doi.org/10.1016/j.neuro.2007.02.004.
52. **Danilchanka O, Pavlenok M, Niederweis M.** 2008. Role of porins for uptake of antibiotics by *Mycobacterium smegmatis*. Antimicrob Agents Chemother **52:**3127–3134. http://dx.doi.org/10.1128/AAC.00239-08.
53. **Niederweis M.** 2003. Mycobacterial porins—new channel proteins in unique outer membranes. Mol Microbiol **49:**1167–1177. http://dx.doi.org/10.1046/j.1365-2958.2003.03662.x.
54. **Hoffmann C, Leis A, Niederweis M, Plitzko JM, Engelhardt H.** 2008. Disclosure of the mycobacterial outer membrane: cryo-electron tomography and vitreous sections reveal the lipid bilayer structure. Proc Natl Acad Sci U S A **105:**3963–3967. http://dx.doi.org/10.1073/pnas.0709530105.
55. **Djoko KY, Goytia MM, Donnelly PS, Schembri MA, Shafer WM, McEwan AG.** 2015. Copper(II)-bis(thiosemicarbazonato) complexes as antibacterial agents: insights into their mode of action and potential as therapeutics. Antimicrob Agents Chemother **59:**6444–6453. http://dx.doi.org/10.1128/AAC.01289-15.
56. **Gengenbacher M, Kaufmann SH.** 2012. *Mycobacterium tuberculosis*: success through dormancy. FEMS Microbiol Rev **36:**514–532. http://dx.doi.org/10.1111/j.1574-6976.2012.00331.x.
57. **Miura G.** 2015. Antibacterials: stressing out dormancy. Nat Chem Biol **12:**1. http://dx.doi.org/10.1038/nchembio.1992.
58. **Olaleye O, Raghunand TR, Bhat S, Chong C, Gu P, Zhou J, Zhang Y, Bishai WR, Liu JO.** 2011. Characterization of clioquinol and analogues as novel inhibitors of methionine aminopeptidases from *Mycobacterium tuberculosis*. Tuberculosis (Edinb) **91**(Suppl 1):S61–S65. http://dx.doi.org/10.1016/j.tube.2011.10.012.
59. **Lewis K.** 2013. Platforms for antibiotic discovery. Nat Rev Drug Discov **12:**371–387. http://dx.doi.org/10.1038/nrd3975.
60. **Dragset MS, Poce G, Alfonso S, Padilla-Benavides T, Ioerger TR, Kaneko T, Sacchettini JC, Biava M, Parish T, Arguello JM, Steigedal M, Rubin EJ.** 2015. A novel antimycobacterial compound acts as an intracellular iron chelator. Antimicrob Agents Chemother **59:**2256–2264. http://dx.doi.org/10.1128/AAC.05114-14.
61. **Di Vaira M, Bazzicalupi C, Orioli P, Messori L, Bruni B, Zatta P.** 2004. Clioquinol, a drug for Alzheimer's disease specifically interfering with brain metal metabolism: structural characterization of its zinc(II) and copper(II) complexes. Inorg Chem **43:**3795–3797. http://dx.doi.org/10.1021/ic0494051.
62. **Nakamura M, Kitamura C, Ueyama H, Yamana K, Yoneda A.** 2005. Crystal structure of 8-hydroxyquinoline-2-carboxylic acid copper(II) complex. Anal Sci X-ray Struct Anal Online **21:**x115–x116. http://dx.doi.org/10.2116/analscix.21.x115.
63. **Tardito S, Barilli A, Bassanetti I, Tegoni M, Bussolati O, Franchi-Gazzola R, Mucchino C, Marchiò L.** 2012. Copper-dependent cytotoxicity of 8-hydroxyquinoline derivatives correlates with their hydrophobicity and does not require caspase activation. J Med Chem **55:**10448–10459. http://dx.doi.org/10.1021/jm301053a.
64. **Stahl C, Kubetzko S, Kaps I, Seeber S, Engelhardt H, Niederweis M.** 2001. MspA provides the main hydrophilic pathway through the cell wall of *Mycobacterium smegmatis*. Mol Microbiol **40:**451–464. http://dx.doi.org/10.1046/j.1365-2958.2001.02394.x.
65. **Mailaender C, Reiling N, Engelhardt H, Bossmann S, Ehlers S, Niederweis M.** 2004. The MspA porin promotes growth and increases antibiotic susceptibility of both *Mycobacterium bovis* BCG and *Mycobacterium tuberculosis*. Microbiology **150:**853–864. http://dx.doi.org/10.1099/mic.0.26902-0.
66. **Haas KL, Franz KJ.** 2009. Application of metal coordination chemistry to explore and manipulate cell biology. Chem Rev **109:**4921–4960. http://dx.doi.org/10.1021/cr900134a.
67. **Field TB, McCourt JL, McBryde WAE.** 1974. Composition and stability of iron and copper citrate complexes in aqueous solution. Can J Chem **52:**3119–3124. http://dx.doi.org/10.1139/v74-458.
68. **Amolegbe SA, Adewuyi S, Akinremi CA, Adediji JF, Lawal A, Atayese AO, Obaleye JA.** 2015. Iron(III) and copper(II) complexes bearing 8-quinolinol with amino-acids mixed ligands: synthesis, characterization and antibacterial investigation. Arabian J Chem **8:**742–747. http://dx.doi.org/10.1016/j.arabjc.2014.11.040.
69. **Xiao Z, Brose J, Schimo S, Ackland SM, La Fontaine S, Wedd AG.** 2011. Unification of the copper(I) binding affinities of the metallo-chaperones Atx1, Atox1, and related proteins: detection probes and affinity standards. J Biol Chem **286:**11047–11055. http://dx.doi.org/10.1074/jbc.M110.213074.
70. **Foster AW, Osman D, Robinson NJ.** 2014. Metal preferences and metallation. J Biol Chem **289:**28095–28103. http://dx.doi.org/10.1074/jbc.R114.588145.
71. **Rae TD, Schmidt PJ, Pufahl RA, Culotta VC, O'Halloran TV.** 1999. Undetectable intracellular free copper: the requirement of a copper chaperone for superoxide dismutase. Science **284:**805–808. http://dx.doi.org/10.1126/science.284.5415.805.
72. **Foster AW, Robinson NJ.** 2011. Promiscuity and preferences of metallothioneins: the cell rules. BMC Biol **9:**25. http://dx.doi.org/10.1186/1741-7007-9-25.